Published in final edited form as:
Biomacromolecules. 2013 July 8; 14(7): 2326–2331. doi:10.1021/bm400618m.

Peptide fibrils with altered stability, activity, and cell selectivity

Long Chen and **Jun F. Liang***
Department of Chemistry, Chemical Biology, and Biomedical Engineering, Charles V. Schaefer School of Engineering and Sciences, Stevens Institute of Technology, Hoboken, NJ 07030, USA

Abstract

Peptides have some unique and superior features compared to proteins. However, the use of peptides as therapeutics is hampered by their low stability and cell selectivity. In this study, a new lytic peptide (CL-1, FLGALFRALSRLL) was constructed. Under the physiological condition, peptide CL-1 self-assembled into dynamically stable aggregates with fibrils-like structures. Aggregated CL-1 demonstrated dramatically altered activity and stability in comparison with single molecule CL-1 and other lytic peptides: when incubated with co-cultured bacteria and tissue cells, CL-1 aggregates killed bacteria selectively but spared co-cultured human cells; CL-1 aggregates kept intact in human serum for more than five hours. Peptide-cell interaction studies performed on lipid monolayers and live human tissue cells revealed that in comparison with monomeric CL-1, aggregated CL-1 had decreased cell affinity and membrane insertion capability on tissue cells. A dynamic process involving aggregate dissociation and rearrangement seemed to be an essential step for membrane bound CL-1 aggregates to realize its cytotoxicity to tissue cells. Our study suggests that peptide aggregation could be as important as the charge and secondary structure of a peptide in affecting peptide-cell interactions. Controlling peptide self-assembly represents a new way to increase the stability and cell selectivity of bioactive peptides for wide biomedical applications.

Keywords

Antibacterial peptides; Self-assembly; Aggregation; Stability; Cell selectivity

Introduction

Peptides regulate many physiological processes, acting at some sites as endocrine or paracrine signals, and at others as neurotransmitters or growth factors. Bioactive peptides have a positive impact on the functions and conditions of living organisms and show several useful properties for human health, including antimicrobial, antifungal, antiviral, and antitumor activities[1–3]. In addition, peptides with more unique and exciting biological functions, such as cell penetrating[4, 5] and tumor homing[6, 7], have been identified and being applied in wide pharmaceutical and biomedical applications over the last decade. There has been a rapid expansion in the study of peptides, and this is likely to continue.

*Correspondence author. Dr. Jun F. (James) Liang, Department of Chemistry, Chemical Biology, and Biomedical Engineering, Stevens Institute of Technology, Castle Point on Hudson, Hoboken, NJ 07030, USA, Tel.: 201-216-5640; Fax: 201-216-8240, jliang2@stevens.edu.

Peptides have some unique and superior features compared to proteins. However, the widespread use of peptides as therapeutics is hampered mainly by their rapid elimination from the circulation. Typically, peptides are cleared from the bloodstream through renal filtration (for peptides < 5 kDa), enzymatic degradation, and uptake by the reticuloendothelial system (RES)[8]. Because most therapeutic peptides are rich in lysine and arginine residues, they are very sensitive to various proteases, and thus have very short life-span in the circulation which is usually insufficient for peptides to be fully exposed to the target tissue. Approaches such as D-amino acid replacement, polymer conjugation, and microparticulate encapsulation have been tried[9–11]. Unfortunately, D-amino acid replacement and polymer conjugation may be associated with dramatic peptide activity drop. Microparticulate encapsulations are accompanied by increased peptide retention in RES to yield undesired toxicity to spleens and livers.

Peptide self-assembly is a spontaneous arrangement of peptides into a rather stable stage under thermodynamic equilibrium conditions through non-covalent interactions. Self-assembling into aggregates in solutions is a common phenomenon for many peptides[12–17]. Depending on their charges, sequences, secondary structures, and solvation properties, therapeutic peptides may self-assemble into huge peptide aggregates with defined nanostructures. An obvious example is β-amyloid (Aβ) peptides which can self-assemble to make up of long, insoluble ordered fibers, the main constituent of amyloid plaques in the brains of Alzheimer's disease patients[16, 17].

In this study, we reported that the self-assembled bioactive peptide had dramatically improved stability. Both the stability and activity of bioactive peptides could be manipulated and peptide self-assembly provided a great way to tune not only the stability but also the activity and selectivity of bioactive peptides.

Materials and Methods

Materials

All peptides for this study (> 90% in purity) were synthesized by Genescript Corporation (Piscataway, NJ). 1, 2-dipalmitoyl-sn-glycero-3-phosphocholine (DPPC), 1, 2-dipalmitoylsn-glycero-3-phospho-(1'-rac-glycerol) (sodium salt) (DPPG) and 1, 2-dihexadecanoyl-sn-glycero-3-phospho-L-serine (sodium salt) (DPPS) were purchased from Avanti Polar Lipid, Inc. (Alabaster, Alabama). A LIVE/DEAD bacteria staining kit was purchased from Invitrogen Life Technologies (Carlsbad, CA). All human cell lines and bacteria were obtained from American Type Culture Collection (ATCC, Manassas, VA). All other chemicals were purchased from Sigma–Aldrich Co. (St. Louis, MO).

Methods

Antibacterial Activity Assay—Bacteria was grown in tryptic soy broth (TSB) supplemented with 0.2% glucose (TSBG)[18]. Peptides stock solution was serially diluted in a buffer containing 0.2% bovine serum albumin (BSA) and 0.01% acetic acid. Samples of each concentration (10 μl/well) were added in the wells of 96-well plates (Costar, Cambridge, MA), followed by bacterial cell suspensions (90 μl/well). Midlogarithmic (mid-

log) phase bacteria at a final concentration of ~ 2×10^6 cells/ml in the medium were used. The minimal inhibitory concentrations (MIC) were defined as the lowest concentration of peptide that completely prevented bacteria growth (OD570nm) over 20 hours of incubation at 37 °C.

Cytotoxicity Measurement—The cytotoxicity of peptides was determined using Thiazolyl Blue Tetrazolium Bromide (MTT) assay as described previously[15, 19]. Briefly, cells in complete medium were added into 96-well plates (5×10^3 cells/well) and cultured at 37 °C for 14–16 hours. After being washed, cells were fed with serum-free F12K medium containing various concentrations of peptides and incubated at 37 °C for 2 hours. After that, 10 μl of MTT (5 mg/ml) was added into each well. Cell viability was determined after 4 hours of incubation by dissolving crystallized MTT with 10% sodium dodecyl sulfate solution containing 5% isopropanol and 0.1% HCl and measuring absorbance at 570 nm.

Measurement of Peptide-Induced Surface Tension Changes[15]—Peptide-induced surface tension change on the lipid monolayer was recorded on a Microtrough X (Kibron Inc., Philadelphia, PA). A lipid mixture of DPPC–cholesterol–DPPS (50/10/2.5) or DPPC–DPPG (50/3), to mimic mammalian cell or bacteria cell membrane, was dissolved in 3:1 chloroform–methanol to form 100 μM lipid solutions. To a four-well teflon plate, 1.0 ml PBS was added, followed by a drop of lipid solution. A lipid monolayer was formed on the water surface after the evaporation of organic solvent. Peptide-induced surface tension change was recorded right after peptide solutions were added to the subphase through the side pores of the teflon plate. When the monolayer surface area is fixed, there will be a rapid surface tension increase as peptides bind to the lipid monolayer. If the peptide binding is associated with peptide insertion into the lipid monolayer, surface tension will show a biphasic behavior: a rapid tension increase is followed by a gradual decline. The second phase surface tension decrease reflects peptide insertion-induced rearrangement of lipid molecules in the monolayer.

Peptide Degradation in Human Sera—Peptides (final concentration = 10 μM) were incubated with 1.0 ml pooled human sera and incubated at 37 °C. At indicated time points, peptide samples were collected and then purified through ZipTip-C18 column (Millipore Co., Billerica, MA). The amount of intact peptide was determined using matrix-assisted laser desorption/ionization-time of-flight (MALDI-TOF) mass spectrometry. The matrix used was α-cyano-4-hydrocinnamic acid (10 mg/ml in 50% acetonitrile with 0.05% trifluoroacetic acid). Appropriate molecular weight standards (New England Biolabs Inc. Ipswich, MA) were used to calibrate the instrument. Measurements were made on Bruker UltraFlextreme mass spectrometer and data were analyzed with Flex analysis version 3.3 software (Bruker Daltonik GmbH Co., Billerica, MA).

Acquisition of Peptide Circular Dichroism (CD) Spectra[20]—The CD spectra of peptides were recorded on a Jasco J-710 spectropolarimeter. The CD spectra were scanned at 25 °C in a capped, quartz optical cell with a 1.0 mm path length. Data were collected from 250 to 190 nm at an interval of 1.0 nm with an integration time of two seconds at each wavelength. Five to ten scans were averaged, smoothed, background-subtracted, and

converted to mean residue molar ellipticity [θ] (degrees cm^2 $dmol^{-1}$) for each measurement. CDPRO software was used to analyze the data obtained from the CD spectropolarimeter.

Electron Microscopy—Freshly prepared and overnight incubated peptides (80 μM) were loaded on silicon wafers for 30 minutes at 37 °C, and then washed with deionized water. Samples were coated with gold[21]. SEM images were taken by Auriga Modular CrossBeam workstation (Carl Zeiss Inc., Thornwood, NY).

The overnight cultured peptide CL-1 was also deposited onto carbon grids for TEM imaging. After being washed with deioninzed water, the sample was stained with uranyl acetate. Images were taken by TEM (Model CM20, Philips, Eindhoven, Netherlands).

Kinetic Studies of Peptide-induced Cell Membrane Damage Using LIVE/DEAD Kit[21]—Freshly trypsinized human lung carcinoma A549 cells were seeded in a collagen-coated 8-well glass chamber (2×10^4 cells/well) and cultured in F12K medium containing 10% FBS at 37 °C (5% CO_2) overnight. Before the assay, cells were washed with PBS three times and stained with the LIVE/DEAD staining kit for 15 min. After the addition of peptides, cell images were recorded at different time points using a Zeiss LSM510 Confocal Microscope (Carl Zeiss Inc., Thornwood, NY). The excitation wavelength was fixed at 488 nm and the emission wavelengths were set at 505–530 nm (for the live cells) and 560 nm (for the dead cells). The percentage of green pixels out of total green and red pixels in captured cell images was calculated to estimate the cell membrane integrity.

Peptide Aggregates Measurement and Characterization—Peptides from stock solutions (5 mM in water/DMSO mixture) were diluted with PBS, and incubated at 37 °C for 18 hours. Peptide aggregation were characterized using three methods: i) The sizes of peptide aggregates in solutions were measured using a Zeta nanosizer (Malvern Instruments, Worcestershire, United Kingdom) at indicated time[21]; ii) Formation of peptide aggregation in the solutions was estimated using a fluorescence probe 1-anilinonaphthalene-8-sulfonic acid (1, 8-ANS). ANS (20 μM) fluorescence emission spectrum increase caused by peptide aggregation was recorded on a fluorescence Microplate Reader (Biotek Inc.) by setting excitation wavelength at 369 nm[15]; iii) The binding of Congo Red (CR) to peptide amyloid fibrils was associated with CR absorption spectrum changes. The concentration of CR was fixed at 5 μM while peptide concentrations changed in the range of 0~80 μM. CR absorption spectra were recorded on a microplate reader[15, 22].

Co-culture of Bacteria and Mammalian Cells[18]—*Staphylococcus aureus* (ATCC 25923) suspended in 100 μl F12K supplemented with 10% (v/v) fetal bovine serum was added directly onto A549 cell monolayers cultured in the wells of 8-well glass chamber. The final concentration of *S. aureus* was controlled at 10^3 bacteria per well. Peptides were added at final concentrations of 20 μM. Cells were incubated at 37 °C in a humidified atmosphere of 5% CO_2 for 6 hours. At the end of incubation, cells were washed with saline and then stained using LIVE/DEAD kit. Stained cells were visualized under a Zeiss LSM 510 confocal microscopy.

Results and Discussions

Lytic peptides are a group of cationic peptides which kill cells by causing cell lysis[15]. Because both the targeting and acting sites are located on cell membranes, lytic peptides kill cells without the needs of getting into the cells. As a result, lytic peptides are active to both antibiotic sensitive and resistant bacteria, including MRSA[18, 23]. PTP-7 (FLGALFKALSKLL) is a well studied lytic peptide with proved antibacterial activity to antibiotic resistant bacteria[20].

It was reported that peptides with specific sequences could self-assemble into aggregates with regular structures[24, 25]. We constructed a PTP-7 derivative, CL-1 (FLGALFRALSRLL), by replacing the two lysine residues at position #7 and position #11 with arginines, an important amino acid which directly involved in peptide self-assembly and aggregation[26, 27]. There are two reasons for such lysine→arginine substitutions: 1) we have proven that the two positive charges at position #7 and position #11 are essential in order to maintain the cell lysis activity of resulting peptides[18–20]; 2) unlike lysine and histidine, arginine has a complex guanidinium group. Because of the conjugation between the double bond and the nitrogen lone pairs, the positive charge on the side chain of arginine is delocalized. Charge delocalization on side chain will allow arginine residues to form varied and multiple inter-molecule hydrogen bonds to facilitate peptide aggregation.

Although both PTP-7 and CL-1 aggregated in solution at high concentrations, only CL-1 formed profound, large (> 2.0 μm), and dynamically stable peptide aggregates after long time (> 4–6 hours) of incubations. CL-1 aggregation was confirmed in different assays established in our previous studies[21] using DSL, 1,8-ANS and Congo red (Figure 1). Like all other peptides, CL-1 aggregation was concentration dependent. CL-1 formed β-amyloid type aggregates as indicated by the red shift of Congo red absorbance spectra (Figure 1A). CL-1 aggregates formed easily when high concentrations of CL-1 peptide were used. In any cases, initially formed peptide aggregates were unstable and had continuously changed aggregate sizes. Dynamically stable CL-1 aggregates were formed after extended (overnight or > 8 hrs) incubation (Figure 1B). Although dynamically stable CL-1 aggregates could be precipitated by high speed centrifugation, re-suspension of precipitated CL-1 would give the same size aggregates after a brief sonication treatment. Quantitative aggregation analysis using DLS and congo red revealed that 90–95 % of CL-1 in solution existed as aggregates after overnight incubation.

Aggregates from peptide CL-1 was sensitive to acidic pH and dissolved rapidly (< 30 minutes) and completely when the solution pH was adjusted from the physiological pH to the pH=5.5 (Figure 1 B & 1C). CL-1 was unable to form aggregates at acidic pH even at very high peptide concentrations and after long time of incubation. The pH sensitivity of peptide aggregates implied the involvement of inter-peptide hydrogen bonds in peptide aggregations. Because guanidinium group can form varied and multi hydrogen bonds, it explains the dramatic aggregation of CL-1 peptide. It should be pointed out that solution pH in the range of 5.5–7.5 had no dramatic effect on guanidinium groups (pKa=12.5) of arginine residues. However, pH change from 7.5 to 5.5 could dramatically affect the

protonation of terminal NH_2 and COOH, and thus the equilibrium between NH_3^+-peptide-COO^- and NH_2-peptide-COOH in solutions.

The SEM study revealed that aggregation of PTP-7 was not significant. Few small size peptide aggregates (100~200 nm in size) were found (Figure 2A). However, aggregation of peptide CL-1 at the same concentration as PTP-7 was very profound (Figure 2B). CL-1aggregates were a mixture of nano-size particles (up to 200 nm in sizes) and fibers. Long chain fibrils of micro-meters in length from self-assembled CL-1 formed dense networks with regular structures (Figure 2C). Formation of fibril network explained the size difference of CL-1 aggregates as measured using Nanosizer (average 2.5 μm) (Figure 1) and SEM (< 200 nm) (Figure 2B).

In order to test the effect of self-assembly on peptide stability, we incubated PTP-7 and CL-1 peptides with human sera and monitored peptide degradation using mass spectrometry. We know that peptide bonds from arginine and lysine have close sensitivity to enzymes in human plasma. However, self-assembled peptide CL-1 demonstrated excellent biological stability. Aggregated CL-1 remained intact (> 95%) after 5 hours of incubation while peptide PTP-7 was completely degraded (Figure 3). Aggregated peptide CL-1 had an estimated half-life of 8–9 hours. On the contrary, freshly prepared and not aggregated CL-1 sample with no or little aggregation (Figure 1) showed close stability as peptide PTP-7, confirming that self-assembly was the direct reason for the increased stability of peptide CL-1.

We had proven that PTP-7 was a very potent antibacterial peptide which could cause bacterial cell lysis within 30 minutes of incubation[18]. In order to investigate the potential effect of aggregation on the activity of peptides, the antimicrobial activities of PTP-7 and CL-1 were compared against a group of bacteria (Table 1). Surprisingly, self-assembling hardly affected the antibacterial activity of CL-1. Aggregated CL-1 gave the same or comparable MIC values as PTP-7 and non-aggregated CL-1 on all tested bacteria.

Because lytic peptides have their primary targets on the cell membrane and display activity that is on the borderline between those of venom-like peptides (cytotoxin class III) and antibacterial peptides, lytic peptides show very potent antimicrobial activity to antibiotic-resistant bacteria including methicillin-resistant *S. aureus* (MRSA) by inducing bacterial cell lysis[18, 23]. This makes lytic peptides very attractive for their potential applications in the treatment of various infectious diseases in which antibiotic resistance has already developed. Unfortunately, because the lipid bilayer is the most conservative part of the cell and all living organisms have the same lipid bilayer membrane structures, lytic peptides usually can not distinguish bacteria from the host cells and thus demonstrate unacceptable toxicity for clinical applications[28, 29].

Like other lytic peptides, PTP-7 has strong cytotoxicity to tissue cells by causing cell membrane lysis[15, 20]. Interestingly, peptide CL-1 demonstrated low cytotoxicity. The IC_{50} value of peptide CL-1 was about 10 times higher than that of PTP-7 (Figure 4). However, if CL-1 aggregates were first dissolved in acidic solution (Figure 1) or when freshly prepared CL-1 was used, peptide CL-1 showed comparable IC_{50} value with PTP-7 (IC_{50} = 9 μM and

14 μM for PTP-7 and freshly prepared CL-1, respectively). Obviously, unlike PTP-7 and free CL-1, self-assembled CL-1 had dramatically increased bacteria selectivity (IC_{50}/MIC ratio=16–18).

It is known that lytic peptide interactions with cell membranes include three thermodynamic steps: 1) the electrostatic attraction of cationic peptides to anionic cell membranes; 2) the transition of the peptide into the plane of binding and accumulation on the surfaces of cell membranes; and 3) the insertion of concentrated peptides into cell membranes to induce cell lysis. The electrostatic attraction of cationic peptides to the cell membranes is the PTP-7 CL-1 critical step which is solely determined by the net positive charges of a peptide. In addition, the folding of the peptide chain into a specific conformation, usually an alpha-helical structure, has proven to be a necessary and energy favorable process for peptide insertion into cell membranes[15]. By replacing two lysine residues with arginines, resulting peptide CL-1 had the same positive charges (+2) as PTP-7. In addition, peptide CL-1 maintained the same secondary structures as PTP-7 (Figure 5). Both peptides existed as random coil in solution but adopted α-helical structures when they encountered hydrophobic environments like that in the lipid bilayer of cell membranes. Therefore, neither charge nor secondary structure contributed directly to the observed activity difference of CL-1 to bacteria and human tissue cells.

We then compared PTP-7 and CL-1 binding and insertion into the lipid monolayer on a micro trough. PTP-7 gave typical membrane insertion curves on both tissue (Figure 6A) and bacterial (Figure 6B) cell membrane mimics which were characterized by an initial phase of rapid surface tension increase, followed by a second phase of surface tension relaxation. The Phase I and phase II surface tension changes represented peptide binding to and insertion into the lipid monolayer, respectively. In comparison with PTP-7, freshly prepared CL-1 showed slightly decreased membrane insertion capability but had increased binding affinity to both tissue and bacterial cell membrane mimics (tension change = 17 vs 12 mN/m and 11 vs 9 mN/m for CL-1 and PTP-7 on tissue and bacterial cell membrane mimics, respectively). Although aggregated CL-1 acted the same as the non-aggregated peptide on bacterial cell membrane mimic in terms of membrane binding and insertion (Figure 6B), it behaved differently from non-aggregated CL-1 on tissue cell membrane mimic (Figure 6A): 1) aggregated CL-1 had decreased binding affinity (tension change dropped from 17 mN/m to 13 mN/m); 2) aggregated CL-1 demonstrated reduced membrane insertion capability as reflected by the flat tension relaxation curve. Obviously, aggregation affected both CL-1 binding and insertion into cell membranes. Altered peptide-membrane interactions explain the low human cell toxicity and thus the bacteria selectivity of aggregated CL-1 peptide.

Dynamic studies of cell membrane lysis using LIVE/DEAD dye staining revealed that PTP-7 caused rapid tissue cell lysis and completed within 25 minutes. However, CL-1 induced cell membrane damage was a slow process and did not reach 100% cell lysis even after long time (120 minutes) of incubation (Figure 7A). Dramatically reduced acting time was observed for peptide CL-1 if acidic culture media were used in the cytotoxicity assay to dissolve peptide aggregates (Figure 7B).

The bacterial selectivity of CL-1 peptides was further confirmed in a cytotoxicity analysis performed on bacterium and human cell co-cultures (Figure 8). In the assay, *S. aureus* (10^3 cfu/ml) was added onto cultured A549 (human lung cells) cell monolayer. Toxins released from *S. aureus* caused immediate A549 cell death (Figure 8B) and almost all A549 cells were dead and stained red by Live/Dead kit after 6 hours of incubation. Although adding peptide PTP-7 into the co-cultures successfully inhibited the bacteria growth, it induced severe damage to the co-cultured A549 cells (Figure 8C). We did not observe cytotoxicity difference between overnight incubated (Figure 8C) and freshly (Figure 8E) prepared PTP-7. However, if the same concentration of overnight cultured CL-1 was added, only *S. aureus* were selectively killed and co-cultured A549 cells were spared (Figure 8D). More than 80% of A549 cells were still alive after incubation with peptide CL-1 for 6 hours. The same bacterial selectivity was not found for freshly prepared and non-aggregated CL-1. Freshly prepared CL-1 acted similarly as peptide PTP-7 and caused severe tissue cell damages (Figure 8F).

Conclusions

Self-assembling into aggregates with defined structures is a common phenomenon for most peptides[13, 14]. Impacts of peptide self-assembly on peptide-cell interaction have been revealed in recent publications[21, 30]. Results from this study suggest that peptide aggregation could be as important as the charge and secondary structure of a peptide in affecting peptide-cell interactions. Controlling peptide self-assembly may represent a new way to increase the stability and cell selectivity of bioactive peptides for wide biomedical applications as we had demonstrated in this study.

Acknowledgments

This work was supported by National Institutes of Health grant GM081874 and AI072748. Mr. Chen is a recipient of the innovation and entrepreneurship doctoral fellowship.

References

1. Zhang G, Yin X, Qi Y, Pendyala L, Chen J, Hou D, Tang C. Curr. Cardiol. Rev. 2010; 6:62–70. [PubMed: 21286280]
2. Bidwell GL. Ther. Delivery. 2012; 3:609–621.
3. Nguyen LT, Haney EF, Vogel HJ. Trends Biotechnol. 2011; 29:464–472. [PubMed: 21680034]
4. Cardoso AM, Trabulo S, Cardoso AL, Lorents A, Morais CM, Gomes P, Nunes C, Lúcio M, Reis S, Padari K, Pooga M, Pedroso, de Lima MC, Jurado AS. Biochim. Biophys. Acta. 2012; 1818:877–888. [PubMed: 22230348]
5. Lim S, Kim WJ, Kim YH, Choi JM. Mol. Cells. 2012; 34:577–582. [PubMed: 23263658]
6. Xiao M, Hong Z, Sun L, Wu Y, Zhang N, Liu Y, Luo D, Zhou J, Li C. J. Huazhong Univ. Sci. Technol. Med. Sci. 2011; 31:608–613. [PubMed: 22038348]
7. Hamzah J, Kotamraju VR, Seo JW, Agemy L, Fogal V, Mahakian LM, Peters D, Roth L, Gagnon MK, Ferrara KW, Ruoslahti E. Proc. Natl. Acad. Sci. U. S. A. 2011; 108:7154–7159. [PubMed: 21482787]
8. Green BD, Gault VA, Mooney MH, Irwin N, Harriott P, Greer B, Bailey CJ, O'Harte FP, Flatt PR. Bio.l Chem. 2004; 385:169–177.
9. Janek K, Rothemund S, Gast K, Beyermann M, Zipper J, Fabian H, Bienert M, Krause E. Biochemistry. 2001; 40:5457–5463. [PubMed: 11331010]

10. Ricci M, Giovagnoli S, Blasi P, Schoubben A, Perioli L, Rossi C. Int. J. Pharm. 2006; 311:172–181. [PubMed: 16439072]
11. Ibrahim MA, Ismail A, Fetouh MI, Göpferich A. J. Controlled Release. 2008; 106:241–252.
12. Subbalakshmi C, Manorama SV, Nagaraj R. J. Pept. Sci. 2012; 18:283–292. [PubMed: 22431418]
13. Meng Q, Kou Y, Ma X, Liang Y, Guo L, Ni C, Liu K. Langmuir. 2012; 28:5017–5022. [PubMed: 22352406]
14. Castelletto V, Cheng G, Hamley IW. Chem. Commun. (Camb). 2011; 47:12470–12472. [PubMed: 22042055]
15. Chen L, Tu Z, Voloshchuk N, Liang JF. J. Pharm. Sci. 2012; 101:1508–15017. [PubMed: 22227945]
16. Larini L, Shea JE. Biophys. J. 2012; 103:576–586. [PubMed: 22947874]
17. Bowerman CJ, Nilsson BL. Biopolymers. 2012; 98:169–184. [PubMed: 22782560]
18. Kharidia R, Tu Z, Chen L, Liang JF. Arch Microbiol. 2011; 194:579–685.
19. Chen L, Liang JF. Eur. J. Pharm. Biopharm. 2012; 81:339–345. [PubMed: 22487054]
20. Tu Z, Volk M, Shah K, Clerkin K, Liang JF. Peptides. 2009; 30:1523–1528. [PubMed: 19464332]
21. Chen L, Patrone N, Liang JF. Biomacromolecules. 2012; 13:3327–3333. [PubMed: 22934601]
22. Klunk WE, Jacob RF, Mason RP. Anal. Biochem. 1999; 266:66–76. [PubMed: 9887214]
23. Steinstraesser L, Hauk J, Schubert C, Al-Benna S, Stricker I, Hatt H, Shai Y, Steinau HU, Jacobsen F. PLoS One. 2011; 6:e18321. [PubMed: 21483840]
24. Zhao X, Zhang S. Macromol. Biosci. 2007; 7:13–22. [PubMed: 17225214]
25. Scanlon S, Aggeli A. Nano Today. 2008; 3:22–30.
26. Liberato MS, Kogikoski S, Silva ER, Coutinho-Neto MD, Scott LP, Silva RH, Oliveira VX, Ando RA, Alves WA. J. Phys. Chem. B. 2013; 117:733–740. [PubMed: 23286315]
27. Kawasaki T, Kamijo S. Biosci. Biotechnol. Biochem. 2012; 76:762–766. [PubMed: 22484947]
28. Yates C, Sharp S, Jones J, Topps D, Coleman M, Aneja R, Jaynes J, Turner T. Biochem. Pharmacol. 2011; 81:104–110. [PubMed: 20869347]
29. Hansel W, Enright F, Leuschner C. Mol. Cell. Endocrinol. 2007:260–262. 183–189.
30. Wadhwani P, Strandberg E, Heidenreich N, Bürck J, Fanghanel S. J. Am. Chem. Soc. 2012; 134:6512–6515. [PubMed: 22452513]

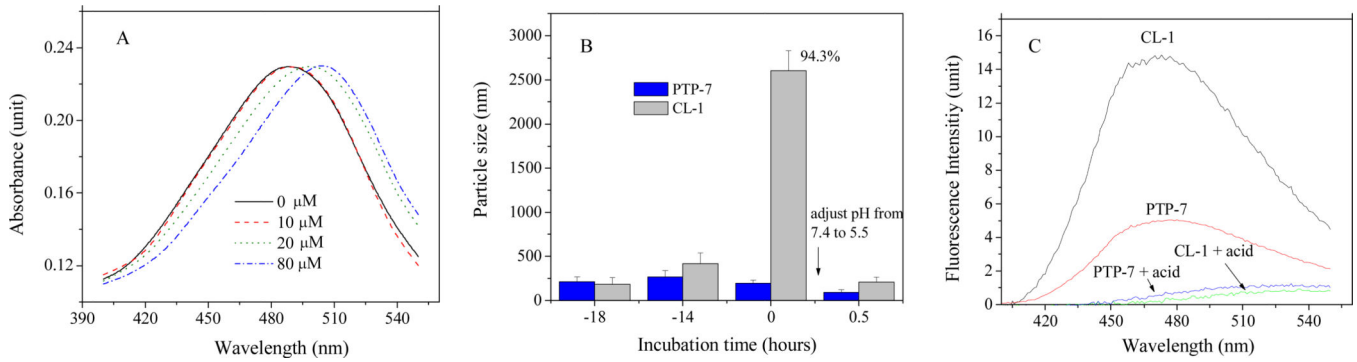

Figure 1.

A) Absorbance spectra of Congo red in the presence of 0–80 μM CL-1 at pH = 7.4, PBS. Absorbance was normalized to highlight the red shift upon peptide addition; B) Kinetics of peptide aggregation in PBS (pH=7.4) solutions. CL-1 aggregates dissolved immediately after HCl was added and the solution pH was adjusted to 5.5. Sizes of peptide aggregates were measured using Nanosizer. Nearly 95% of CL-1 in solutions existed as aggregates after overnight incubation as indicated; C) Aggregation of overnight incubated CL-1 and PTP-7 was measured using 1, 8-ANS by setting excitation wavelength at 369 nm. Peptide and 1, 8-ANS concentrations were fixed at 80 μM and 20 μM, respectively. Before measurements, peptide samples were subjected to a brief (60 seconds) sonication treatment.

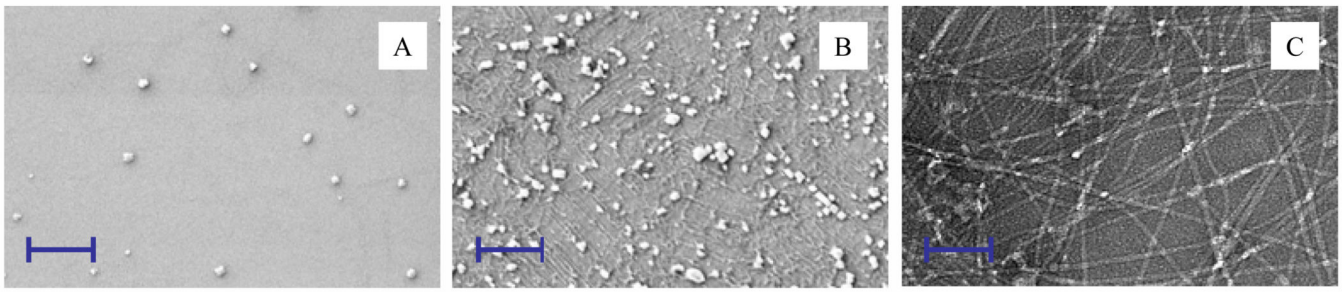

Figure 2.

A) SEM image of peptide PTP-7; B) SEM image of peptide CL-1; C) TEM image of CL-1. Peptides (80 μM in water) were incubated at 37 °C overnight. In SEM analysis, the solutions were deposited onto a piece of silicon wafer for 30 minutes and washed with deionized water to remove salts. Samples were coated with gold before taking the SEM images. In TEM analysis, the solution was deposited onto a carbon grid and stained with uranyl acetate. Scale bar = 1.0 μm.

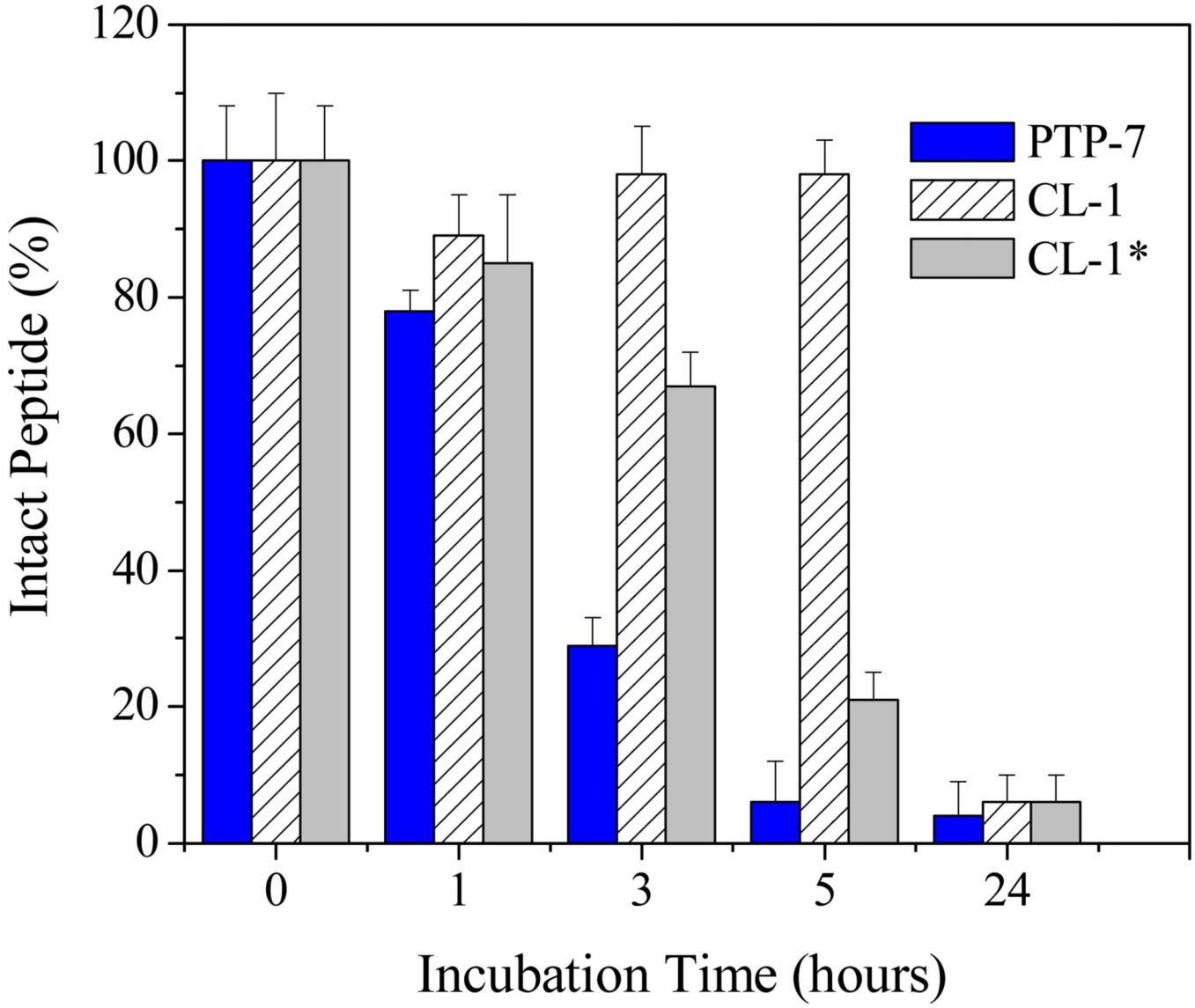

Figure 3.

Kinetics of peptide degradation in human sera. Peptides (10 μM) were incubated with 1.0 ml pooled human sera at 37 °C. Intact peptide at the indicated time points was determined using MALDI-TOF mass spectrometry. CL-1* refers to freshly prepared sample from completely dissolved (non-aggregated) CL-1.

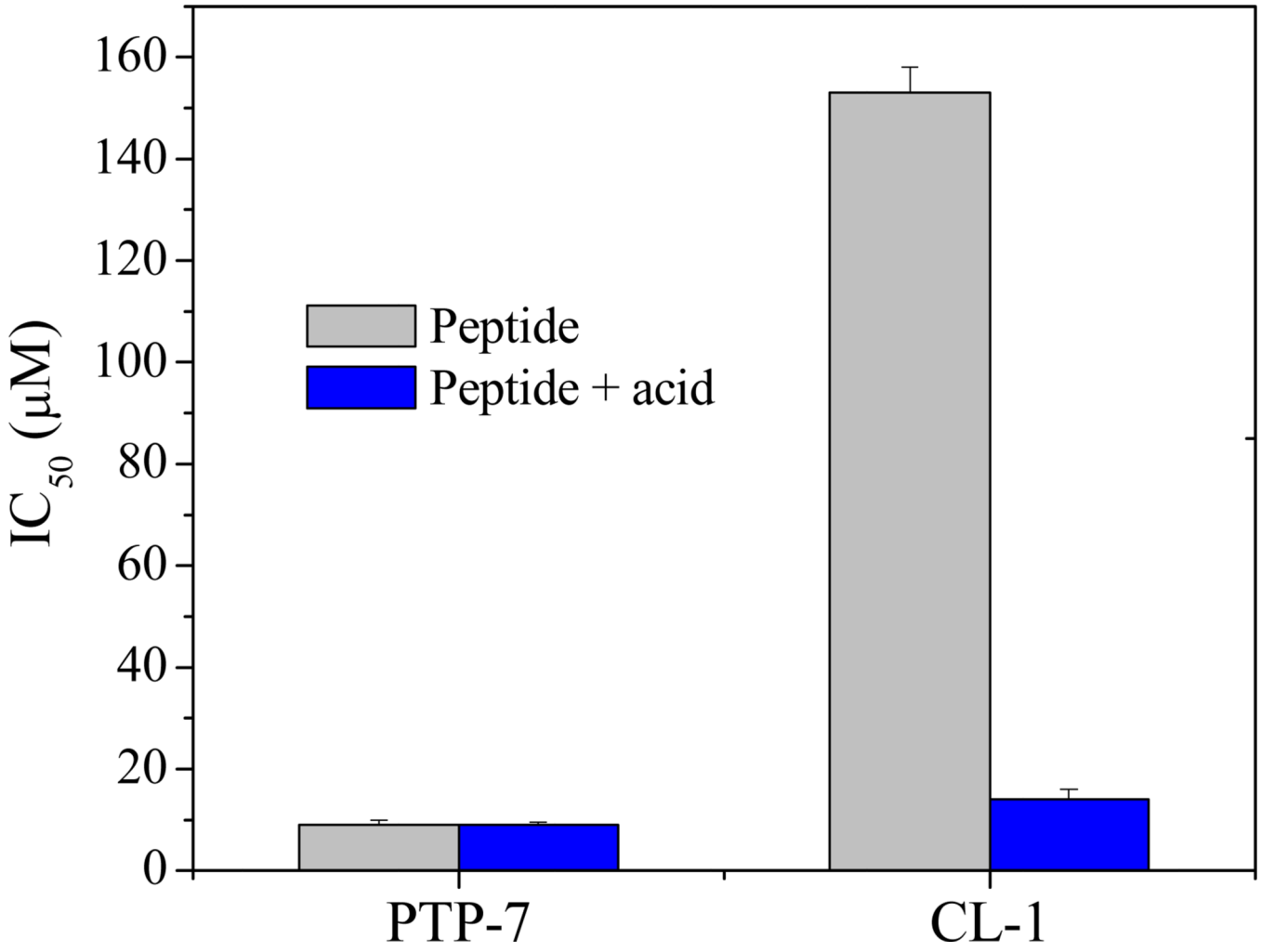

Figure 4.

Overnight incubated peptide in pH=7.4 and acidic (pH=5.5) solutions were added into cultured A549 cells in 96-well plates. Cell viability was measured using MTT assay after two hours of incubation. CL-1 aggregates completely dissolved in pH=5.5 PBS.

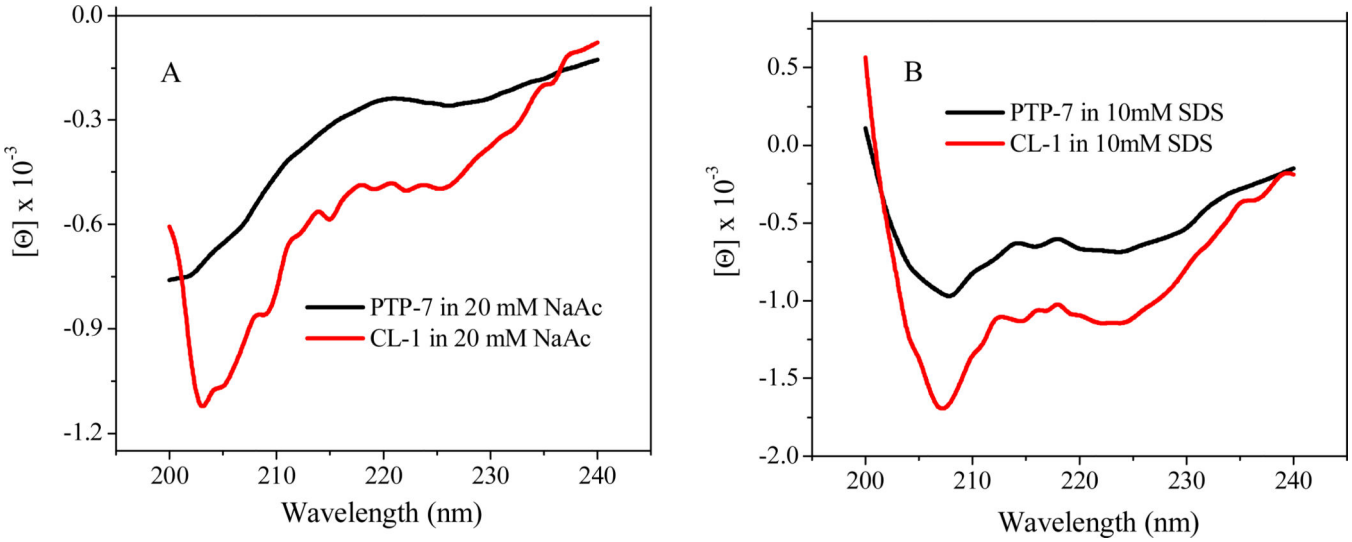

Figure 5.

CD spectra of peptide PTP-7 and CL-1 in 20 mM NaAc (A) and 10 mM SDS (B) solutions at pH=7.4.

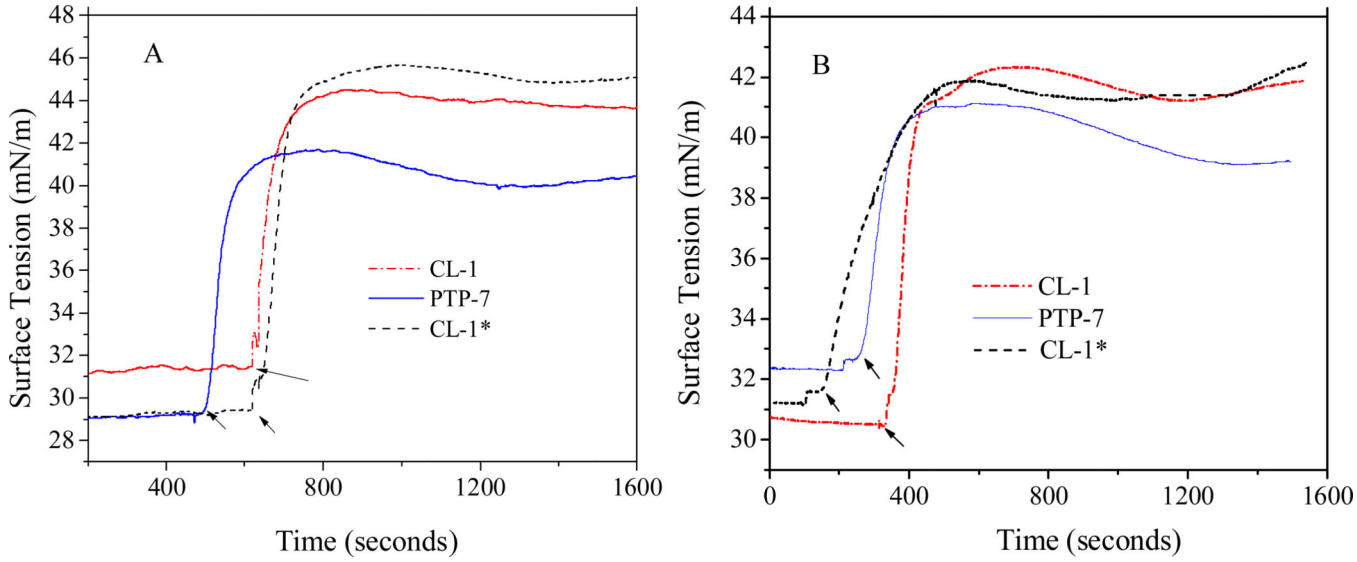

Figure 6.

Peptide binding and insertion associated surface tension changes of lipid monolayer mimicking tissue cell (DPPC/Cholesterol/DPPS=50/10/2.5) (A) and bacteria (DPPC// DPPG=50/3) (B) membranes. CL-1* refers to freshly prepared sample from completely dissolved (non-aggregated) CL-1. The initial surface tension of lipid monolayer was set at about 30 mN/m. The final peptide concentrations were kept at 10 μM. The time points of peptide loading were indicated by arrows.

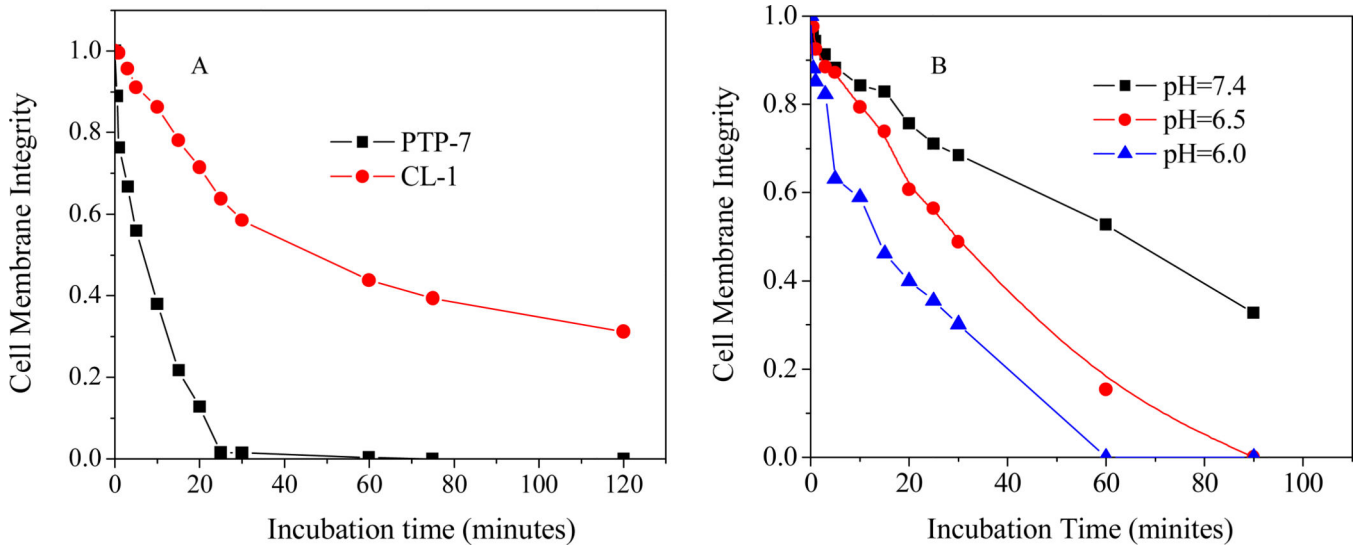

Figure 7.

A) Dynamics of peptide PTP-7 and CL-1 induced cell membrane permeation to LIVE/DEAD dyes; B) The pHs affected cell lysis activity of peptide CL-1. Fluorescence images were taken at different time points after peptide solutions were added. The percentage of green pixels out of the total green and red pixels was calculated to estimate the cell membrane integrity.

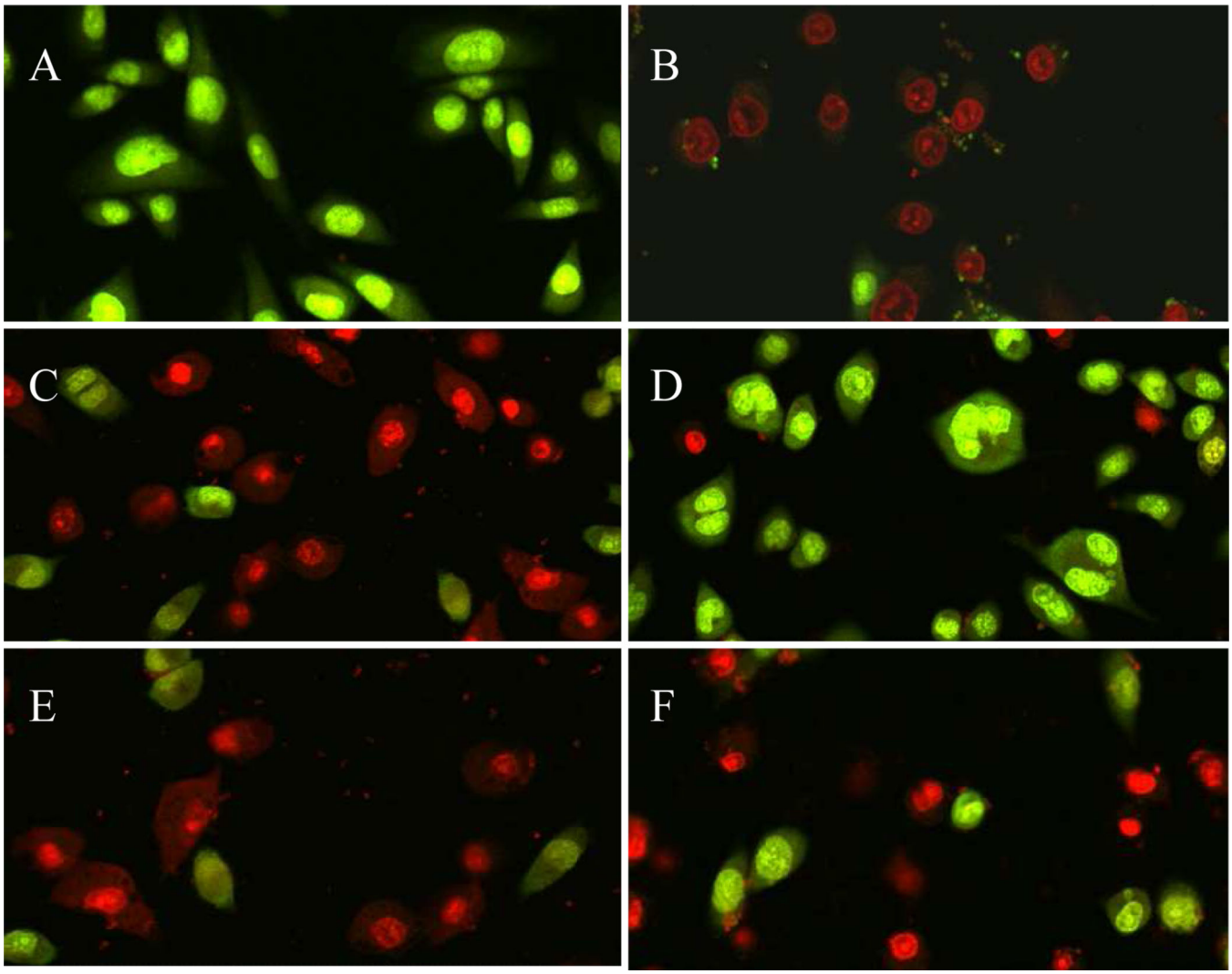

Figure 8.

Confocal microscopy images of bacterium and mammalian cell co-cultures. *S. aureus* (25923, 10^3 cfu/ml) were added into cultured A549 cell monolayer and incubated for 6 hours in the absence or presence of peptides. A) A549 cell alone; B) A549 cells + *S. aureus*; C) A549 cells + *S. aureus* + 20 μM overnight incubated PTP-7; D) A549 cells + *S. aureus* + 20 μM overnight incubated CL-1; E) A549 cells + *S. aureus* + 20 μM freshly prepared PTP-7 from completely dissolved PTP-7; F) A549 cells + *S. aureus* + 20 μM freshly prepared CL-1 from completely dissolved (non-aggregated) CL-1. Live A549 cells were stained green while dead A549 cells were stained red or yellow by using Live/Dead kit.

Table 1

Antimicrobial activities (MIC, μg/ml) of peptide PTP-7 and CL-1

	***S aureus* (25923)**	***S. aureus* (29213)**	***S. Epidermidis* (35984)**
PTP-7	4	8	8
CL-1	8	8	4
CL-1*	8	8	8
Penicillin G	1	16	4

CL-1* refers to freshly prepared sample from completely dissolved (non-aggregated) CL-1.